A Journal of the Gesellschaft Deutscher Chemiker

Angewandte Chemie

GDCh

International Edition

www.angewandte.org

Accepted Article

Title: Versatile Three-dimensional Porous Cu@Cu2O Aerogels Networks as Electrocatalysts and Mimicking Peroxidases

Authors: Pinghua Ling, Qiang Zhang, Tingting Cao, and Feng Gao

To be cited as: *Angew. Chem. Int. Ed.* 10.1002/anie.201801369
Angew. Chem. 10.1002/ange.201801369

Link to VoR: http://dx.doi.org/10.1002/anie.201801369
http://dx.doi.org/10.1002/ange.201801369

WILEY-VCH

Versatile Three-dimensional Porous Cu@Cu_2O Aerogels Networks as Electrocatalysts and Mimicking Peroxidases

*Pinghua Ling, Qiang Zhang, Tingting Cao, Feng Gao**

[*] P. Ling, Q. Zhang, T. Cao, Prof. Dr. F. Gao*

Laboratory of Functionalized Molecular Solids, Ministry of Education, Anhui Key Laboratory of Chemo/Biosensing, Laboratory of Optical Probes and Bioelectrocatalysis (LOPAB), College of Chemistry and Materials Science, Anhui Normal University, Wuhu 241002, P. R. China

E-mail: fgao@mail.ahnu.edu.cn.

Supporting information for this article is given via a link at the end of the document.

Abstract

Much attention has been focused on self-or directed-assembling nanoparticles into three-dimensional porous nanostructures due to their collective performances and unexpected applications. In this study, we report a facile strategy to form three-dimensional (3D) porous Cu@Cu_2O aerogels networks by self-assembling Cu@Cu_2O nanoparticles with the diameters of ca. 40 nm for constructing catalytic interfaces. Unexpectedly, the prepared Cu@Cu_2O aerogels networks display excellent electrocatalytic activity to glucose oxidation at a low onset potential of ca. 0.25 V. Moreover, the Cu@Cu_2O aerogels also can act as mimicking-enzymes including horseradish peroxidase and NADH peroxidase, and show obvious enzymatic catalytic activities to the oxidation of dopamine (DA), o-phenyldiamine (OPD), 3,3,5,5-tetramethylbenzidine (TMB), and dihydronicotinamide adenine dinucleotide (NADH) in the presence of H_2O_2. The designed 3D Cu@Cu_2O aerogels networks in this study may represent a new class of porous catalytic materials as mimic peroxidases and electrocatalysts and offer a novel platform to construct catalytic interfaces for promising applications in electrochemical sensors and artificial enzymatic catalytic systems.

10.1002/anie.201801369

Introduction

In recent years, self- or directed-assembling nanoparticles into one-, two-, and three-dimensional porous nanostructures with collective properties such as high electrocatalytic activity or mimicking-enzyme functions has attracted growing interest.[1] Some metal oxide nanoparticles[2] such as MnO_2, Cu_2O, Fe_3O_4, metal nanoparticles,[3] alloy nanomaterials,[4] metal-organic frameworks,[5] Cu^{2+}-modified graphene oxide nanoparticles,[6] Cu^{2+}-modified carbon nitride or carbon dots,[7] hemin-modified peptides,[8] and hemin/G-quadruplex[9] have been reported to mimic the functions of horseradish peroxidase (HRP) for bioanalytical applications or used as electrocatalysts to construct non-enzymatic electrochemical sensors. However, some nanoparticles are easily aggregated or oxidized in the ambient atmosphere, which thus limits their catalytic activities and further applications in different areas. Obviously, it is still a challenge and highly desired to develop facile and environmental-friendly approaches to assembly nanosized entities with unique optical and electronic properties into macroscopic nanostructures endowed with the abilities of high electrocatalytic activity or mimicking-enzyme.

Among the developed nanostructures, the porous nanostructures have attracted much attention in the catalytic systems due to their large surface area, abundant active sites, high stability and good solubility. As highly porous materials, aerogels possess fascinating structures such as ultralow density, large surface area, open interconnected pores, various composition and size, and morphology effect.[10] Compared to traditional porous materials, the aerogels display unique electronic, catalytic, and optical characteristics, and thus have been explored for a wide range of applications.[11] In particular, the noble metal nanoparticles based aerogels have been widely exploited. For example, Au hydrogel networks with the dopamine-induced 3D assembly of Au NPs have been designed for electrocatalytic oxidation of glucose.[12] Multimetallic hierarchical aerogels, Ni-Pd_xPt_y, have also been reported for efficient electrocatalysis of ethanol oxidation.[13] However, these original metal nanoparticles are cost-expensive and therefore restrict their further applications. The 3D porous aerogels networks as assembled with cheap metal Cu or their oxide nanoparticles have been rarely reported so far for electrocatalysts and mimicking enzymes.

In this work, a facile strategy has been developed for designing multifunctional 3D Cu@Cu_2O aerogels networks, which may represent a new class of biomimetic catalytic materials as mimic peroxidases and heterogeneous electrocatalysts to the oxidation of some small molecules. As shown in Scheme 1, the 3D Cu@Cu_2O aerogels networks exhibit electrocatalysis toward glucose oxidation with high sensitivity and excellent selectivity. And also, the 3D Cu@Cu_2O aerogels networks show distinguished peroxidase-like catalytic activities to the oxidation of a variety of substrates including dopamine (DA), o-phenyldiamine (OPD), 3,3,5,5-tetramethylbenzidine (TMB), and dihydronicotinamide adenine dinucleotide (NADH) in the presence of H_2O_2. The versatile catalytic functions of 3D Cu@Cu_2O aerogels networks could broaden the scope of Cu_2O applicability in bioanalysis and pave a new platform for constructing electrochemical sensing systems.

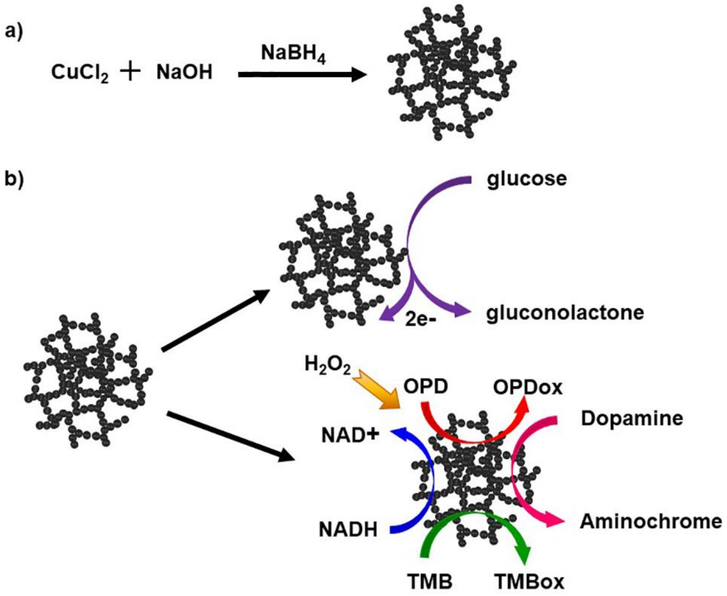

Scheme 1. Schematic illustration of a) the preparation, and b) versatile biomimetic catalytic properties of 3D Cu@Cu_2O aerogels networks.

Results and discussion

The nanoscaled 3D Cu@Cu_2O aerogels networks were synthesized with one simple step through the redox reaction of the mixed aqueous solution of NaOH and $CuCl_2$ with fresh $NaBH_4$ solution under strong stirring at room temperature. The obtained products were collected by centrifugation with water and ethanol, respectively, and then dried at room temperature. It is worthy to note that the present method is simple, rapid, stable, easy operation, and wild preparation conditions without any heating steps, compared with other methods.[14] The 3D Cu@Cu_2O aerogels networks are firstly examined using scanning electron microscopy (SEM). The SEM images shown in Figure 1a indicate that the 3D structures are highly porous and composed of interconnected networks of ultrathin spongy-like structures. High-magnification SEM image (inset of Figure 1a) depicts that the prepared network-like nanostructures are composed of nanoparticles with a mean size of ca. 40 nm.

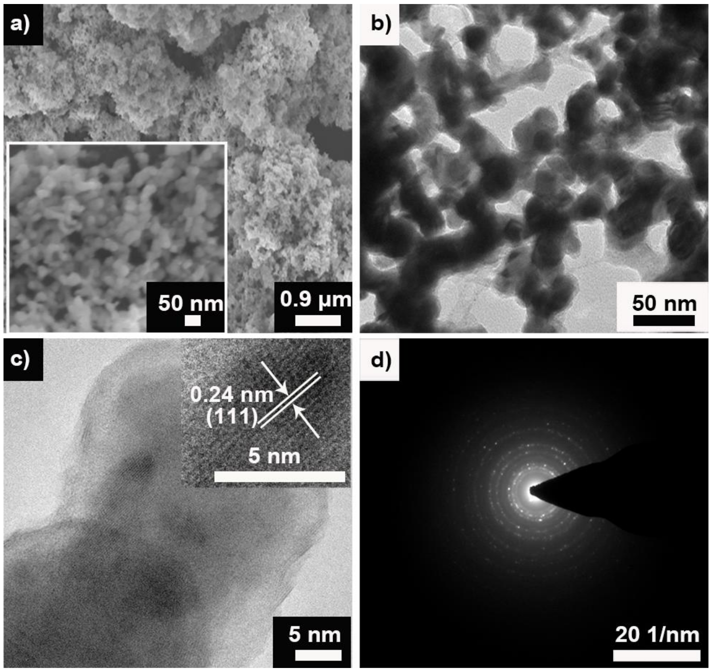

Figure 1. a) SEM images (inset: high-magnification SEM morphology). b) low-magnification TEM images. c) high-resolution TEM (inset: The interplanar spacing of high-resolution TEM). d) selected area electron diffraction pattern of Cu@Cu_2O aerogels networks.

The size and the composition of the prepared 3D Cu@Cu_2O aerogels networks were further characterized using transmission electron microscopy (TEM) and energy-dispersive X-ray spectroscopy (EDX). The TEM (Figure 1b) shows that Cu@Cu_2O aerogels are formed into network-like morphologies and the formed nanoparticles are approximately 40 nm in diameter, which are consistent with the SEM results. The EDX spectra (Figure S1) and percentage analysis of elements in Cu@Cu_2O (Table S1) indicate that these Cu@Cu_2O aerogels are mainly composed of Cu and a little amount of O. The absorption bands at 450-510 nm in the UV-vis spectrum suggest that the formation of Cu_2O (Figure S2A) in the preparation of aerogels.[14a] The Fourier transform infrared spectrum (Figure S2B) shows no other obvious peaks except for the absorption bands of H_2O and CO_2, suggesting that these prepared Cu@Cu_2O aerogels are very pure and are suitable to investigate the catalytic activities. The high-resolution TEM (Figure 1c) and selected area electron diffraction pattern (Figure 1d) reveal the diffraction rings and the polycrystalline nature of Cu@Cu_2O aerogels.

To verify the purity and phase of 3D Cu@Cu_2O aerogels networks, the XRD are characterized and shown in Figure 2a. The XRD peaks (2θ) at 36.4^o, and 61.3^o are agreed well with the (111) and (220) reflections of Cu_2O (JCPDS no. 78-2076), respectively. Moreover, three diffraction peaks located at 43.3^o, 50.4^o and 74.1^o are indexed to the (111), (200) and (220) of the face centered cubic (fcc) of Cu (JCPDS no. 04-0836), respectively, and ascribed to the pure phase of its bulky sample. In order to confirm the element information of the Cu@Cu_2O aerogels networks, the X-ray photoelectron spectroscopy (XPS) was also carried out. As shown in Figure 2b, the XPS survey spectrum of Cu2p shows the typical bands at 932.4 eV and 952.2 eV, respectively, which are the typical characteristic of Cu_2O and can be attributed to Cu/Cu_2O (Cu^0/Cu^+).[15] Whereas, the presence of peaks located at 934.0 and 954.1 eV confirm the presence of CuO/$Cu(OH)_2$ (Cu^{2+}).[16] The weak satellite peaks at 941.1 eV, 943.5 eV and 962.1 eV are corresponded to the Cu^{2+}, and attributed to the open $3d^9$ shell of Cu(II).[16b,17] The tiny amounts of Cu_2O on the surface could be oxidized to CuO and/or $Cu(OH)_2$ species when the surface is exposed in air with humidity.[18] Owing to the different detection sensitivity and detection depth between XPS and XRD, the Cu^{2+}can be detected by the XPS on the Cu_2O, while the CuO and $Cu(OH)_2$ cannot be detected by XRD.[18a,19] In addition, the peak difference between Cu $2p_{3/2}$ (932.4 eV) and Cu $2p_{1/2}$ (952.2 eV) is 19.8 eV, suggesting that Cu^{2+} is present[20] and is consistent with the results of XRD. As shown in Figure 2c, the Auger electron spectrum (Cu $L_3M_{4.5}M_{4.5}$) shows the binding energy peak at 569.8 eV, which is corresponding to the electron state of Cu_2O.[15a] The O1s XPS spectrum (Figure 2d) suggests that O1s is mainly at 531.7 eV, which can be attributed to the absorbed oxygen. The peak at 530.3 eV indicates that oxygen is present in the Cu_2O lattice, while the main peak present at 533.0 eV is attributed to surface species in the Cu@Cu_2O aerogels.[15b] The abundant surface chemical composition and the difference of adsorbed oxygen species may greatly have effects on the catalytic activity of 3D Cu@Cu_2O aerogels networks.[21]

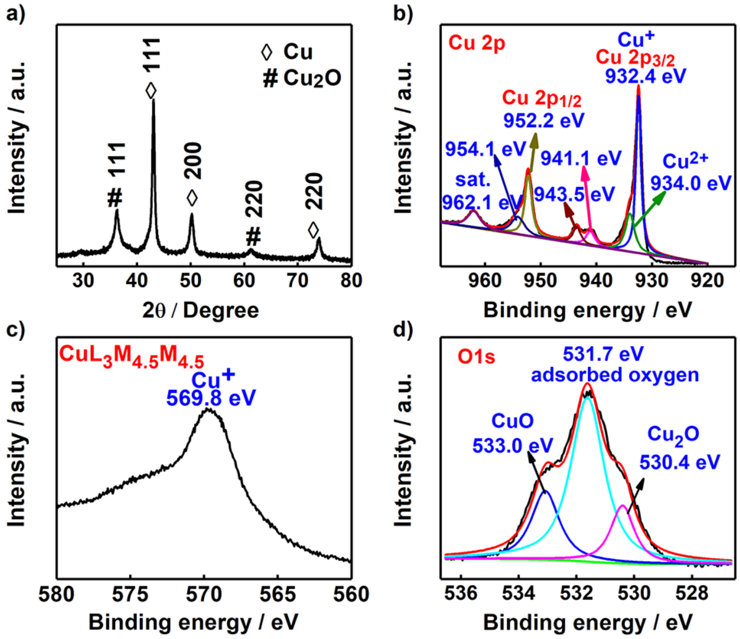

Figure 2. a) XRD pattern, b) XPS spectrum (Cu 2p3/2 core peaks), c) Auger spectrum (Cu $L_3M_{4.5}M_{4.5}$ peak) and d) XPS spectrum (O1s core peaks) of Cu@Cu_2O aerogels networks.

To examine the electrocatalytic behavior of Cu@Cu_2O aerogels towards glucose oxidation, the cyclic voltammogram (CV) measurements were carried out. Figure 3a shows the CVs of the Cu@Cu_2O modified glassy carbon electrode (Cu@Cu_2O/GCE) in 0.1 M NaOH aqueous solution containing various glucose concentrations of 0 mM, 0.1 mM, 0.5 mM and 1.8 mM, respectively, at a scan rate of 50 mV s^{-1} in ambient atmosphere. As shown in Figure 3a, with the increasing in glucose concentration, the anodic currents are gradually enhanced accompanying by the obvious decrease of the cathodic peak currents, which is typical electrocatalytical features. The oxidation of glucose occurs at the onset potential of ca. 0.25 V, which is lower than the value of 0.3 V using metal and metal oxide nanotube network and carbon nanotube-nickel nanocomposites as electrocatalysts,[22] indicating that the 3D Cu@Cu_2Oaerogels networks display highly efficient electrocatalytic activity toward glucose oxidation. The glucose is oxidized to glucolactone in the potential range of 0.25 V to 0.7 V, where the glucose oxidation is catalyzed by Cu(II) to Cu(III) conversion.[23] These phenomena suggest that the Cu(III) specie, rather than Cu(I) or Cu(II), act as an electron mediator in the glucose oxidation.[24] The electrochemical process is followed by chemical catalytic process, in which Cu(I) is first oxidized to $Cu(OH)_2$ species and then transformed to CuO, and CuO is finally oxidized to CuOOH. The redox couple of CuO/CuOOH could catalyze the oxidation of glucose to form gluconolactone, leading to the increasing in anodic currents and decreasing in the cathodic currents.[2c,25]The catalytic mechanisms could be expressed by the following equations.[25]

$$Cu_2O + 3H_2O \longrightarrow 2Cu(OH)_2 + H_2 \quad (1)$$

$$Cu(OH)_2 \longrightarrow CuO + H_2O \quad (2)$$

$$CuO + OH^- \longrightarrow CuOOH + e- \quad (3)$$

$$CuOOH + e- + glucose \longrightarrow CuO + OH^- + gluconolactone \quad (4)$$

Based on the electrocatalytic activity of the Cu@Cu_2O aerogels networks to glucose oxidation, a non-enzymatic glucose sensor has been fabricated. To optimize the poised potential for non-enzymatic glucose sensor with high sensitivity, the amperometric responses of the Cu@Cu_2O/GCE at various potentials ranging from 0.25 to 0.6 V (vs Ag/AgCl) were recorded in 0.1 M NaOH solution with the successive addition of 0.1 mM glucose (Figure S4A). As shown in Figure S4A, with the increasing in applied potential, both the current response and the sensitivity are notably enhanced. However, the background noise currents are also increased with the increased poised potentials. To get the highest sensitivity and avoid the potential interference as possible, 0.55 V was employed as the optimal poised potential for the amperometric measurements, which is lower than that of the Cu_2O nanocubes modified electrode (0.6 V)[14b] and Cu_2O/Cu electrode (0.6 V)[25] for glucose oxidation. In addition, Figure S4B shows good linear correlations between current responses and the glucose concentrations with different poised potentials. The response of glucose concentration was quantified by the chronoamperograms peak current at 0.55 V in Figure 3b. The currents exhibited a good liner relation to the glucose concentration in the range from 50 μM to 8.0 mM with a detection limit of 15 μM at the S/N = 3. The detection of limit was lower than that of the Cu_2O nanocubes based electrode (38 μM)[17b] and Cu_2O/Cu electrode (37 μM)[26] for glucose detection. The potential interfering species in the detection of glucose were also investigated. The amperometric response to the continuous addition of 1.0 mM glucose, followed by 2.5 mM dopamine (DA), 2.5 mM ascorbic acid (AA), 2.5 mM uric acid (UA), 2.5 mM fructose and 2.5 mM lactose at Cu@Cu_2O/GCE was examined in 0.1 M NaOH solution. As presented in Figure S5, the current responses of glucose exhibited remarkable enhancement, whereas the current change for DA, AA, UA, fructose and lactose was negligible. These data demonstrate that the Cu@Cu_2O aerogels show excellent selectivity to electrocatalytic oxidation of glucose and can be used for the detection of glucose in complex samples.

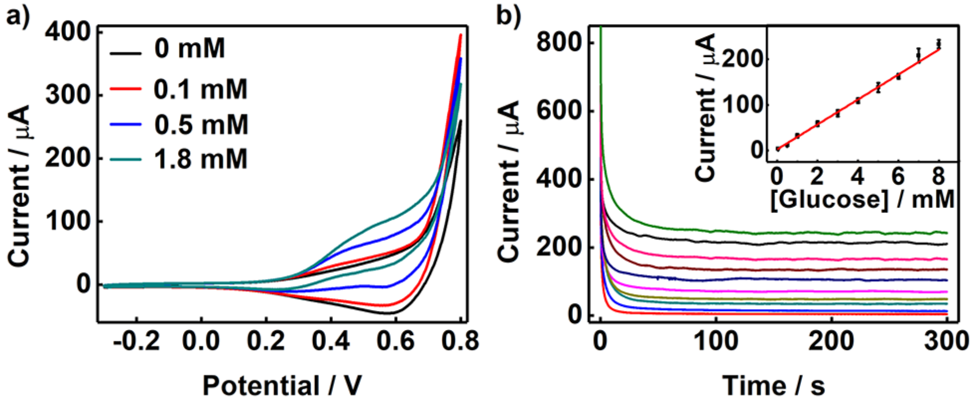

Figure 3. a) CV curves of the Cu@Cu_2O/GCE in a 0.1 M NaOH solution containing 0 mM, 0.1 mM, 0.5 mM and 1.8 mM glucose at a scan rate of 50 mV s^{-1}. b) Chronoamperograms responses of the Cu@Cu_2O/GCE to different glucose concentrations of 0.05 mM, 0.5 mM, 1.0 mM, 2.0 mM, 3.0 mM, 4.0 mM, 5.0 mM, 6.0 mM, 7.0 mM and 8.0 mM (from down to top). Inset: calibration curve of current vs. the concentration of glucose.

Artificial enzymes are very important components of biomimetic chemistry and widely applied in biosensors, immunoassays, cancer diagnostics.[27] In this study, 3D Cu@Cu_2O aerogels with potentially catalytically active centers and exceptionally high water-stability could meet all the prerequisites for a biomimetic system. In order to test the catalytic activity of 3D Cu@Cu_2O aerogels networks as mimic enzymes, we first investigated the mimic peroxidase activity of Cu@Cu_2O aerogels in the DA-H_2O_2 system. As shown in Figure 4a, Cu@Cu_2O aerogels did not show obvious absorption peak, while DA and DA-H_2O_2 systems displayed weak adsorption peak at 480 nm, which is attributed to the oxidation product of dopamine, aminochrome. However, when Cu@Cu_2O aerogels was introduced into DA-H_2O_2 reaction system, the absorption peak at 480 nm was enhanced greatly. This result indicates that the reaction of dopamine and H_2O_2 was catalyzed by Cu@Cu_2O aerogels. The time-dependent absorption spectra and the rates of DA-H_2O_2 in the presence of various concentrations of Cu@Cu_2O aerogels

10.1002/anie.201801369

are shown in Figure S6, from which we can see that the absorbance at the 480 nm increases with the increasing of both the concentration of the Cu@Cu_2O and the reaction time, and the derived V_{max} value reaches a saturation value corresponding to 10 μg mL^{-1} Cu@Cu_2O with a fixed concentration of 5.0 mM dopamine and 10 mM H_2O_2. As the concentration of H_2O_2 increases, the rates of DA oxidation to aminochrome were increased with a fixed concentration of 40 μg mL^{-1} Cu@Cu_2O aerogels and 10 mM dopamine (Figure S7). The reaction rates are also enhanced with the concentrations of DA increase and reach the saturation rate with the DA at ca. 5.0 mM in the presence of 40 μg mL^{-1} Cu@Cu_2O areogels and 10 mM H_2O_2 (Figure S8). The results of the kinetic studies on the DA-H_2O_2-Cu@Cu_2O aerogels reaction system are good agreement with the typical characteristics of enzyme-catalyzed chemical reaction, further suggesting that 3D Cu@Cu_2O aerogels networks could act as the mimetic horseradish peroxidase in the DA-H_2O_2 system.

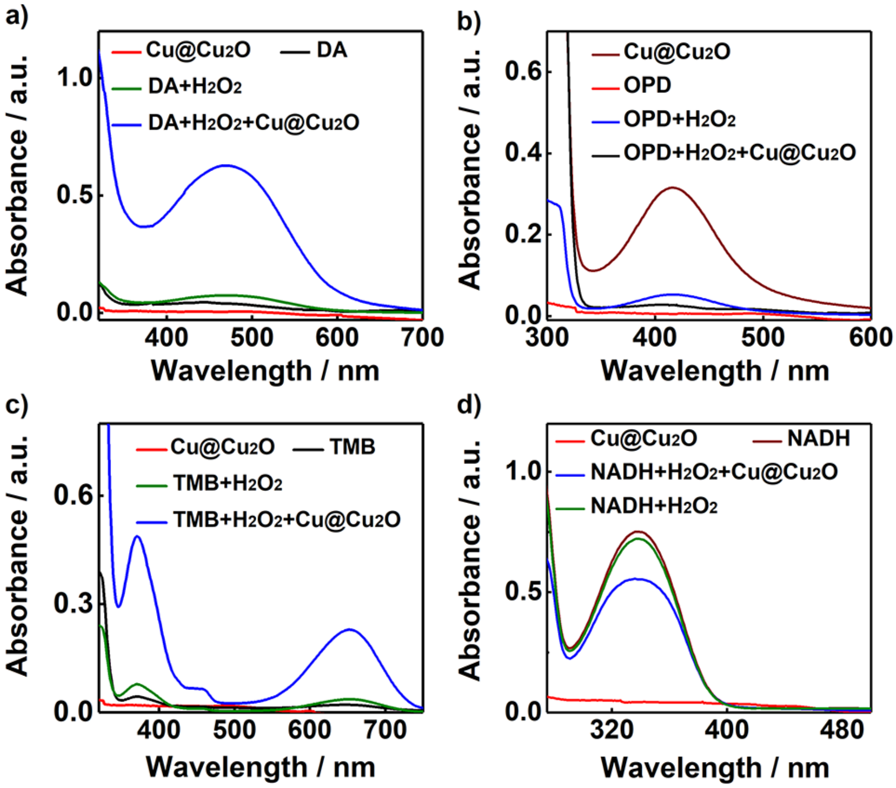

Figure 4. UV-vis absorption spectra of a) DA-H_2O_2, b) OPD-H_2O_2, c)TMB-H_2O_2, and d) NADH-H_2O_2 systems mediated by 3D Cu@Cu_2O aerogels networks. The used concentrations of DA, OPD, TMB, and NADH are all 10 mM, and the concentrations of 3D Cu@Cu_2O aerogels networks and H_2O_2 are 10 μg mL^{-1} and 10 mM, respectively.

In order to further demonstrate the general applicability of 3D Cu@Cu_2O aerogels networks as enzyme mimics, other substrates, such as OPD and TMB, have also been examined, and similar catalytic behaviors are observed. As shown in Figure 4b, for the oxidation of OPD, the absorbance at 420 nm generated from the oxidation product of OPD, phenazine-2,3-diamine, was obviously enhanced when the 3D Cu@Cu_2O networks were added into the OPD-H_2O_2 reaction system. The time-dependent absorbance spectra of phenazine-2,3-diamine generated in the presence of variable concentrations of Cu@Cu_2O aerogels networks with the fixed concentrations of 10 mM OPD and 10 mM H_2O_2 are shown in Figure S9, and the concentration of Cu@Cu_2O aerogels reach a saturation value at 20 μg mL^{-1}. Similarly, the rates of OPD oxidation in the presence of variable concentrations of OPD are depicted in Figure S10, and the V_{max} value reached a plateau at 20 mM. For the oxidation reaction of TMB-H_2O_2 system, the absorbance band at 650 nm originated from the oxidation product of TMB is greatly increased in the presence of Cu@Cu_2O aerogels, as shown in Figure 4c. The rate of TMB oxidation approached a platform at 20 μg mL^{-1} in the present of 1.0 mM TMB and 5 mM H_2O_2, as shown in Figure S11. From Figure S12 and S13, we can see that the rate of TMB oxidation reaches at 10 μg mL^{-1}. All of the above phenomena demonstrate that the Cu@Cu_2O aerogels exhibit excellent horseradish peroxidase-like catalytic activity. The catalytic activity of 3D Cu@Cu_2O aerogels was further investigated in mimicking the NADH peroxidase biocatalytic system. As shown in Figure 4d, comparing to the absorption spectra of NADH, and NADH-H_2O_2, the NADH-H_2O_2-Cu@Cu_2O system displays an obviously decreased absorbance at the 340 nm, indicating that the oxidation of NADH is catalyzed by the

3D Cu@Cu_2O aerogels. In the experiment, we also compare the rate of oxidation of NADH to NAD^+ in the presence of variable concentrations of H_2O_2 or NADH and a fixed concentration of 3D Cu@Cu_2O aerogels. Figure S14 shows that the rates of conversion of NADH to NAD^+ are increased with the increasing concentrations of H_2O_2. Similarly, with the concentration of NADH is increasing, the rates of oxidation of NADH to NAD^+ are enhanced in the presence of Cu@Cu_2O aerogels (20 μg mL^{-1}) (Figure S15). These results demonstrate that the Cu@Cu_2O aerogels also could mimic NADH peroxidase.

In order to get further insights, the enzyme kinetics was employed to study the performances of catalytic activity of the 3D Cu@Cu_2O aerogels networks to the oxidation reactions of different substrates. Based on the different oxidation rates with variable substrate concentrations, nearly ideal hyperbola relationships can be obtained and comply with the classic Michiaelis-Menten equation via nonlinear Hill function simulation[28], as shown in Figure 5. From these plots, some important kinetic parameters including apparent Michaelis−Menten constant (K_m), maximum initial velocity (V_{max}), and catalytic constant (K_{cat}) can be estimated, as summarized in Table 1. The apparent K_m of TMB, OPD, DA and NADH is 0.94 mM, 8.88 mM, 0.47 mM and 0.37 mM, respectively. For the TMB oxidation reaction, the apparent K_m value is lower than the value of 1.63 mM with of zirconium-metalloporphyrin (PCN-222), and 2.448 mM with $Cu(OH)_2$ supercages[29] as mimic peroxidases. Moreover, the apparent K_{cat} values of Cu@Cu_2O with TMB and OPD are higher than the values of 14.0 min^{-1}, 7.3 min^{-1} with PCN-222 and 0.1 min^{-1}, 0.8 min^{-1} with hemin as catalyst, respectively.[5a,30] The fast rate of such a catalytic reaction is ascribed to the high surface area and the exposed activity sits in Cu@Cu_2Oaerogels networks.

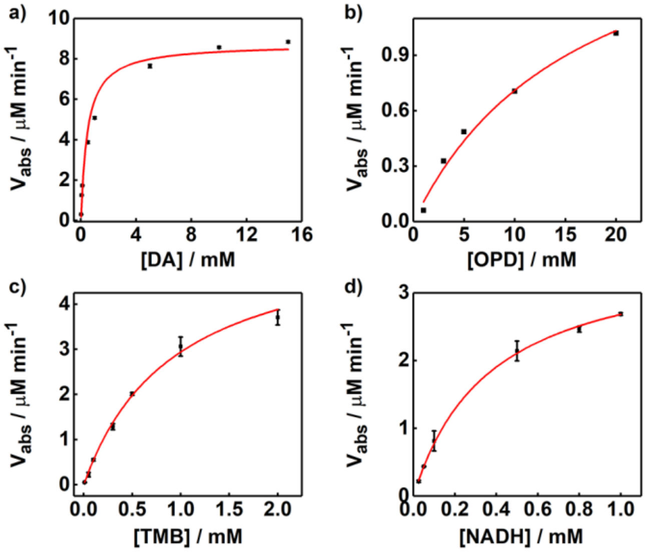

Figure 5. The results of nonlinear fitting of Michaelis-Menten curves for a) DA, b OPD), c) TMB and d) NADH oxidation catalyzed by 3D Cu@Cu_2O aerogels networks.

Table 1. Kinetic parameters of different catalytic oxidation reactions

Substrate	K_m/ mM	V_{max}/ μM min^{-1}	K_{cat}/ min^{-1}	k_{cat}/K_m/ M^{-1} min^{-1}
3,3,5,5-tetrame-thylBenzidine	0.94	5.71	100	1.06×10^5
o-phenylenedi-amine	8.88	1.42	25.00	2.82×10^3
dopamine	0.47	8.73	38.45	8.18×10^4
NADH	0.37	3.68	32.57	8.80×10^4

It is worthy to note that some other sensing systems could also be constructed by directly detecting H_2O_2 or indirectly monitoring generated H_2O_2 on the basis of the excellent peroxidase-like catalytic activity of 3D Cu@Cu_2O aerogels networks for the H_2O_2-involved oxidation reactions. In this study, the detection of glucose by glucose oxidase (GOD)-catalyzed aerobic oxidation is taken as the model system. By probing the UV-vis absorbance at λ = 650 nm of the oxidized product of TMB by H_2O_2 with the catalysis of Cu@Cu_2O aerogels, as demonstrated above. The absorbances can be generated by the oxidation of TMB with the H_2O_2 produced by the GOD-catalyzed aerobic oxidation of variable concentrations of glucose. In these experiments, the oxidation of glucose with variable concentrations is catalyzed by GOD under the aerobic conditions for 30 min at room temperature. The calibration curve shows that the V_{abs} value is increased with the increasing concentration of glucose, which is agreed with the higher concentration of H_2O_2 generated in the biocatalytic system, as shown in Figure S16. Obviously, $Cu@Cu_2O$ aerogels could be applied to sense glucose.

Conclusions

In summary, we provide the first example of $Cu@Cu_2O$ aerogels networks with a diameter of ca. 40 nm as electrocatalytic interfaces for glucose and mimicking horseradish peroxidase and NADH peroxidase. Serving as an electrode material, $Cu@Cu_2O$ aerogels networks modified electrodes exhibit high activities toward the non-enzymatic oxidation of glucose with high sensitivity and excellent selectivity, which could be as a potential platform for the glucose sensors. Furthermore, $Cu@Cu_2O$ aerogels networks exhibit biomimetic catalytic activities and show good catalytic activity to the oxidation of a variety of substrates including DA, OPD, TMB and NADH in the presence of H_2O_2 as HRP and NADH peroxidase. Specifically, glucose sensor can also be constructed by the 3D $Cu@Cu_2O$ aerogels networks based catalysis systems because H_2O_2 could be quantitatively detected by detecting the UV-vis absorbances of the oxidized sate of TMB, in the presence of glucose and glucose oxidase. Future work is focused on examining the cytotoxicity of the $Cu@Cu_2O$ aerogels networks and developing $Cu@Cu_2O$ aerogels networks capable of monitoring intracellular biomolecules.

Acknowledgment

This work was financially supported by National Natural Science Foundation of China (21675084，21575004) and creative research group of bioanalytical chemistry of Anhui Province.

Keywords: $Cu@Cu_2O$ aerogels networks • electrocatalysts • mimicking peroxidases • nanoassembly

References

[1] a) M. J. Stevens, *Science* **2014**, *343*, 981−982; b) L. H. Tan, H. Xing, Y. Lu, *Acc. Chem. Res*. **2014**, *47*, 1881−1890; c) G. X. Ma, Y. L. Zhou, X. Y. Li, K. Sun, S. Q. Liu, J. Q. Hu, N. A. Kotov, *ACSNano* **2013**, *7*, 9010−9018; d) M. R. Gao, S. R. Zhang, Y. F. Xu, Y. R. Zheng, J. Jiang, S. H. Yu, *Adv. Funct. Mater*. **2014**, *24*, 916−924. e) L. L. Sun, Y. M. Fang, Z. M. Li, W. Wang, H. Y. Chen, *Nano Res*. **2017**, *10*, 1740−1748; f) Y. X. Zhao, Y. Zhang, H. Zhao, X. J. Li, Y. P. Li, L. Wen, Z. F. Yan, Z. Y. Huo, *Nano Res.* **2015**, *8*, 2763–2776.

[2] a) H. Wei, E. K. Wang, *Anal. Chem.* **2008**, *80*, 2250−2254; b) F. Natalio, R. Andre, A. F. Hartog, B. Stoll, K. P. Jochum, R. Wever, W. Tremel, *Nat. Nanotechnol*. **2012**, *7*, 530−535; c) C. Q. Dong, H. Zhong, T. Y. Kou, J. Frenzel, G. Eggeler, Z. H. Zhang, *ACS Appl. Mater. Interfaces* **2015**, *7*, 20215−20223.

[3] a) X. X. Zheng, Q. Liu, C. Jing, Y. Li, D. Li, W. J. Luo, Y. Q.Wen, Y. He, Q. Huang, Y. T. Long, C. H. Fan, *Angew. Chem., Int. Ed.* **2011**, *50*, 11994−11998; b) M. B. Gawande, A. Goswami, F. X. Felpin, T. Asefa, X. Huang, R. Silva, X. Zou, R. Zboril, R. S. Varma, *Chem. Rev*. **2016**, *116*, 3722−3811; c) X. H. Kang, Z. B. Mai, X. Y. Zou, P. X. Cai, J. Y. Mo, *Anal. Biochem.* **2007**, *363*, 143−150. d) F. L. Wu , F. R. Cao , Q. Liu , H. Lu, L. Li, *Sci. China Mater*. **2016**, *59*, 825−832.

[4] a) X. J. Zhao, L. Dai, Q. Qin, F. Pei, C. Y. Hu, N. F. Zheng, *small*, **2017**, 13, 1602970; b) M. Vázquez-González, R. M. Torrente-Rodríguez, A. Kozell, W. C. Liao, A. Cecconello, S. Campuzano, J. M. Pingarron, I. Willner, *Nano Lett*. **2017**, *17*, 4958–4963.

[5] a) D. W. Feng, Z. Y. Gu, J. R. Li, H. L. Jiang, Z. W. Wei, H. C. Zhou, *Angew. Chem. Int. Ed*. **2012**, *51*, 10307–10310; b) Y. Chen, T. Hoang, S. Q. Ma, *Inorg. Chem*. **2012**, *51*, 12600−12602; c) X. S. Wang, M. Chrzanowski, D. Q. Yuan, B. S. Sweeting, S. Q. Ma, *Chem. Mater*. **2014**, *26*, 1639−1644.

[6] S. Wang, R. Cazelles, W. C. Liao, M. Vázquez-González, A. Zoabi, R. Abu-Reziq, I. Willner, *Nano Lett*. **2017**, *17*, 2043−2048.

[7] M. Vázquez-González, W. C. Liao, R. Cazelles, S. Wang, X. Yu, V. Gutkin, I. Willner, *ACS Nano* **2017**, *11*, 3247–3253.

[8] a) A. Lombardi, F. Nastri, V. Pavone, *Chem. Rev*. **2001**, *101*, 3165−3190; b) H. M. Marques, *DaltonTrans*. **2007**, 4371−4385; c) H. K. Rau, W. Haehnel, *J. Am. Chem. Soc*. **1998**, *120*, 468−476; d) E. Katz, V. Heleg-Shabtai, I. Willner, H. K. Rau, W. Haehnel, *Angew. Chem., Int. Ed.* **1998**, *37*, 3253−3256; e) M. C. Feiters, A. E. Rowan, R. J. M. Nolte, *Chem. Soc. Rev*. **2000**, *29*, 375−384; f) A. Das, M. H. Hecht, *J. Inorg. Biochem*. **2007**, *101*, 1820−1826.

[9] a) P. Travascio, Y. F. Li, D. Sen, *Chem. Biol.* **1998**, *5*, 505−517; b) P. Travascio, A. J. Bennet, D. Y. Wang, D. Sen, *Chem. Biol*. **1999**, *6*, 779−787.

[10] a) I. U. Arachchige, S. L. Brock, *J. Am. Chem. Soc*. **2006**, *128*, 7964−7971; b) N. Gaponik, A. K. Herrmann, A. Eychmüller, *J. Phys. Chem. Lett*. **2011**, *3*, 8−17; c) H. D. Gesser, P. C. Goswami, *Chem. Rev*. **1989**, *89*, 765−788; d) M. Antonietti, N. Fechler, T. P. Fellinger, *Chem. Mater*. **2014**, *1*, 196−210.

[11] a) I. U. Arachchige, S. L. Brock, *Acc. Chem. Res*. **2007**, *40*, 801−809; b) S. Mahadik-Khanolkar, S. Donthula, A. Bang, C. Wisner, C. Sotiriou-Leventis, N. Leventis, *Chem. Mater*. **2014**, *26*, 1318−1331; c) S. Bag, P. N. Trikalitis, P. J. Chupas, G. S. Armatas, M. G. Kanatzidis, *Science* **2007**, *317*, 490−493; d) W. Liu, A. K. Herrmann, N. C. Bigall, P. Rodriguez, D. Wen, M. Oezaslan, T. J. Schmidt, N. Gaponik, A. Eychmuller, *Acc. Chem. Res*. **2015**, *48*, 154−162.

[12] D. Wen, W. Liu, D. Haubold, C. Z. Zhu, M. Oschatz, M. Holzschuh, A. Wolf, F. Simon, S. Kaskel, A. Eychmuller, *ACS Nano* **2016**, *10*, 2559–2567.

[13] B. Cai, A. Dianat, R. Hübner, W. Liu, D. Wen, A. Benad, L. Sonntag, T. Gemming, G. Cuniberti, A. Eychmüller, *Adv. Mater*. **2017**, 1605254.

[14] a) S. Zhang, Y. Y. Ma, H. Zhang, X. M. Zhou, X. Chen, Y. Q. Qu, *Angew. Chem. Int. Ed.* **2017**, *56*, 8245–8249; b) S. Felix, P. Kollu, B. Raghupathy, S. K. Jeong, A. N. Grace, *J. Chem. Sci*. 2014, 126, 25−32; c) M. Yin, C. K. Wu, Y. B. Lou, C. Burda, J. T. Koberstein, Y. M. Zhu, S. O'Brien, *J. Am. Chem. Soc.* **2005**, *127*, 9506−9511.

[15] a) L. Martin, H. Martinez, D. Poinot, B. Pecquenard, F. L. Cras, *J. Phys. Chem. C* **2013**, *117*, 4421−4430; b) D. A. Svintsitskiy, A. I. Stadnichenko, D. V. Demidov, S. V. Koscheev, A. I. Boronin, *Appl. Surf. Sci.* **2011**, *257*, 8542–8549; c) O. Baghriche, S. Rtimi, C. Pulgarin, R. Sanjines, J. Kiwi, *J. Photochem. Photobiol. A* **2013**, *251*, 50−56; d) D. F. Zhang, H. Zhang, Y. Shang, L. Guo, *Cryst. Growth Des*. **2011**, *11*, 3748−3753.

[16] a) X. Su, J. Zhao, Y. Li, Y. Zhu, X. Ma, F. Sun, Z. Wang, *Colloids Surf. A* **2009**, *349*, 151−155; b) M. A. Brookshier, C. C. Chusuei, D. W. Goodman, *Langmuir* **1999**, *15*, 2043−2046.

[17] a) F. Chen, X. Zhao, H. Liu, J. Qu, *Appl. Catal. B Environ*. **2014**, *158*, 85−90; b) C. C. Chusuei, M. A. Brookshier, D. W. Goodman, *Langmuir* **1999**, *15*, 2806−2808.

[18] Z. Ai, L. Zhang, S. Lee, W. Ho, *J. Phys. Chem. C* **2009**, *113*, 20896−20902.

[19] a) J. Shu, Z. Wang, Y. Huang, N. Huang, C. Ren, W. Zhang, *J. Alloys Compd*. **2015**, *633*, 338−346; b) Q. An, C. Sun, D. Li, K. Xu, J. Guo, C. Wang, *ACS Appl. Mater. Interfaces* **2013**, *5*, 13248−13257.

[20] M. Devaraj, R. Saravanan, R. Deivasigamani, V. K. Gupta, F. Gracia, S. Jayadevan, *J. Mol. Liq*. **2016**, *221*, 930–941.

[21] a) W. Huang, T. Y. Lin, Y. Cao, X. Y. Lai, J. Peng, J. C. Tu, *Sensors* **2017**, *17*, 217–228; b) J. Shu, Z. L. Qiu, S. Z. Lv, K. Y. Zhang, D. P. Tang, *Anal. Chem.* **2017**, *89*, 11135–11142.

[22] a) F. Muench, L. W. Sun, T. Kottakkat, M. Antoni, S. Schaefer, U. Kunz, L. Molina-Luna, M. Duerrschnabel, H. J. Kleebe, S. Ayata, C. Roth, W. Ensinger, *ACS Appl. Mater. Interfaces* **2017**, *9*,

771−781; b) T. Choi, S. H. Kim, C. W. Lee, H, Kim, S. K. Choi, S. H. Kim, E. Kim, J. Park, H. Kim, *Biosens. Bioelectron.* **2015**, *63*, 325–330.

[23] a) L. Zhang, H. Li, Y.H. Ni, J. Li, K. M. Liao, G. C. Zhao, *Electrochem. Commun.* **2009**, *11*, 812–815; b) Y. Qian, F. C. Ye, J. P. Xu, Z. G. Le, *Int. J. Electrochem. Sci.* **2012**, *7*, 10063–10073.

[24] a) H. X. Wu, W. M. Cao, Y. Li, G. Liu, Y. Wen, H. F. Yang, S. P. Yang, *Electrochim. Acta* **2010**, *55*, 3734−3740; b) J. Wang, W. D. Zhang, *Electrochim. Acta* **2011**, *56*, 7510–7516.

[25] a) R. Khan, R. Ahmad, P. Rai, L. W. Jang, J. H. Yun, Y. T. Yu, Y. B. Hahn, I. H. Lee, *Sens. Actuators, B* **2014**, *203*, 471−476; b) J. Jin, G. Zheng, Y. Ge, S. Deng, W. Liu, G. Hui, *Electrochim. Acta* **2015**, *153*, 594−601; d) X. Zhang, G. Wang, W. Zhang, Y. Wei, B. Fang, *Biosens. Bioelectron.* **2009**, *24*, 3395−3398.

[26] L. Wang, J. Y. Fu, H. Q. Hou, Y. H. Song, *Int. J. Electrochem. Sci.* **2012**, *7*, 12587−12600.

[27] a) Y. Fu, X. Y. Zhao, J. L. Zhang, W. Li, *J. Phys. Chem. C* **2014**, *118*, 18116−18125; b) Y. Lin, J. Ren, X. Qu, *Acc. Chem. Res.* **2014**, *47*, 1097−1105; c) H. Wei, E. Wang, *Chem. Soc. Rev.* **2013**, *42*, 6060−6093.

[28] M. H. Chen, F. Li, S. Wang, Y. Cao, *BMC Syst. Biol.* **2017**, *11*, 1−11.

[29] R. Cai, D. Yang, S. J. Peng, X. G. Chen, Y. Huang, Y. Liu, W. J. Hou, S. Y. Yang, Z. B. Liu, W. H. Tan, *J. Am. Chem. Soc.* **2015**, *137*, 13957−13963.

[30] D. I. Metelitsa, O. B. Rus, A. V. Puchkaev, *Russ. J. Appl. Chem.* **1997**, *70*, 1629–16

10.1002/anie.201801369

For Table of Contents Only

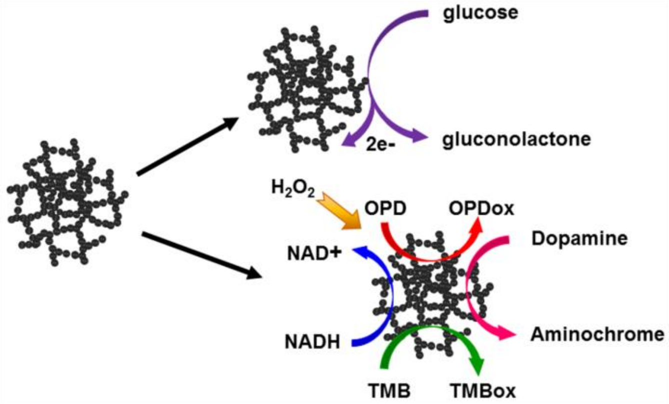

A facile strategy to form three-dimensional (3D) porous Cu@Cu_2O aerogels networks by self-assembling Cu@Cu_2O nanoparticles for constructing catalytic interfaces as electrocatalysts and mimicking peroxidases has been reported. The 3D Cu@Cu_2O aerogels networks exhibit excellent electrocatalysis ability toward glucose oxidation and peroxidase-like catalytic activity to the oxidation of a variety of substrates including dopamine, o-phenyldiamine, 3,3,5,5-tetramethylbenzidine, and dihydronicotinamide adenine dinucleotide in the presence of H_2O_2.